Commun. Comput. Phys.
doi: 10.4208/cicp.OA-2016-0253

Vol. **x**, No. x, pp. 1-11
xxx 201x

Self-Propelled Jump Regime in Nanoscale Droplet Collisions: A Molecular Dynamics Study

Yi Ran Zhang[1], Xi Zhuo Jiang[2], Yi Ran Chen[1] and Kai Hong Luo[1,2,*]

[1] *Center for Combustion Energy, Key Laboratory for Thermal Science and Power Engineering of Ministry of Education, Tsinghua University, Beijing 100084, China.*
[2] *Department of Mechanical Engineering, University College London, Torrington Place, London WC1E 7JE, United Kingdom.*

Received 15 December 2016; Accepted (in revised version) 24 April 2017

Abstract. Self-propelled jump of droplets is among the most striking phenomena in droplet collisions on substrates. Self-propelled jump phenomena of droplets have been observed in experiments, which have also been reproduced in macro- or mesoscale numerical simulations. However, there have been few previous studies on the phenomena at nanoscales. To unravel the dynamics and mechanisms of nanoscale binary droplet collisions on substrates, head-on collision processes of two identical water droplets with diameters of 10nm on graphite substrates are investigated by molecular dynamics (MD) simulations. By varying the impact Reynolds number of binary droplet collisions on hydrophilic or hydrophobic substrates, we successfully reproduce self-propelled jump of droplets on a super-hydrophobic surface with a contact angle of 143° and a relatively high impact Reynolds number of 17.5. Parametric studies indicate that both high impact Reynolds numbers and high hydrophobicity promote self-propelled jump. Moreover, the criterion based on the Ohnesorge number derived from the mesoscopic self-propelled jump regime is insufficient to precisely predict a nanoscale self-propelled jump phenomenon. For this reason, our study includes the impact Reynolds number and the substrate properties like contact angle as additional criteria to refine and extend the current theory for the self-propelled jump behaviours to nanoscales. The study provides insight into the mechanism of self-propelled jump phenomenon at nanoscales.

AMS subject classifications: (or PACS) to be provided by authors

Key words: Self-propelled jump, binary droplet collision, hydrophobic substrates, molecular dynamics.

*Corresponding author. *Email addresses:* K.Luo@ucl.ac.uk (K. H. Luo), zhangyr14@mails.tsinghua.edu.cn (Y. R. Zhang), xizhuo.jiang.14@ucl.ac.uk (X. Z. Jiang), chen-yr14@mails.tsinghua.edu.cn (Y. R. Chen)

1 Introduction

Self-propelled jump of droplet phenomena, depicting that a large droplet formed by binary droplet collisions on a super-hydrophobic surface propels itself to jump away from the surface [1], are frequently encountered in both natural and industrial processes like water-repellent surfaces [2, 3]. These interesting phenomena have been applied to developing functional surfaces which are effective in anti-dew [4], anti-icing [5] or self-cleaning [6]. Despite some successful applications of the phenomena, understanding of the mechanisms associated with the self-propelled jump regime is still preliminary [7, 8]. Experimental and numerical studies using, for example, lattice Boltzmann method (LBM) have already reported self-propelled jump regime in macro- and mesoscales, and their analyses are mostly from the perspectives of energy, without any detailed account of flow dynamics [9, 10]. Details of the nanoscale collision process are difficult to obtain through experiments or continuum simulation methods, especially when the substrate-droplets distance is within a distance comparable to the molecular mean free path. Thus, computer simulations considering atomic effects are currently the only way to reveal droplet dynamics when the substrate-droplet distance comes within nanoscale [11]. Yet up to the present time, the published simulations have not considered the atomic effects. Such an absence is intriguing as it suggests the possibility that the self-propelled jump phenomenon may not exist in nano-droplet collisions on a substrate while it was observed in micro- and macro-droplet collisions.

In this research, molecular dynamics (MD) simulations of water nano-droplet collisions on hydrophobic and hydrophilic substrates will be conducted. By varying the impact Reynolds number and substrate properties like contact angles, we successfully reproduce the self-propelled uprising behaviours under a proper combination of impact Reynolds number and contact angles. Meanwhile, a series of MD simulations will be undertaken to explore the different facets of the self-propelled jump phenomenon.

2 System construction and simulation details

2.1 System construction

To study the distinctive behaviours among hydrophilic and hydrophobic droplets on graphite substrates, three simulation systems were constructed. Each setup comprises two nano-droplets and a double-layer graphite surface, as shown in Fig. 1. The first system is an equilibrium system, and the other two systems aim to study the effects of hydrophobicity on droplet collision behaviours. Therefore, two contact angles between droplets and graphite substrates have been selected to represent different hydrophobicity. The contact angle, θ, of each simulation is 143 and 108 degrees, respectively.

The graphite substrate consists of two square staggered sheets with an interlayer distance of 3.4Å. The side length of each square graphite layer is 500Å. All the carbon atoms are individually fixed at their initial positions to represent an inert substrate. The origin

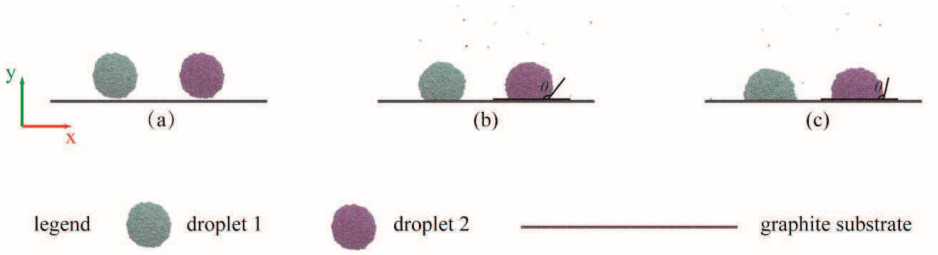

Figure 1: Two nano-droplets on a double-layer graphite substrate. (a) Initial setup of the equilibrium simulation system. (b) Two droplets equilibrated on the substrate with contact angle of 143°. (c) Two droplets equilibrated on the substrate with contact angle of 108°.

of the x direction is set at the left beginning of the graphite layers. Two identical water droplets with diameter of 10nm, were successively placed above the substrate with the distance between their centres of mass (COMs) of 100Å. The whole simulation system comprises 242,340 atoms in total.

2.2 Simulation details

The TIP3P water model [12, 13] was chosen for the intermolecular potential of water molecules. The interactions between water molecules include Coulombic and Lennard-Jones (L-J) potential, and detailed parameters can be referred to [14,15]. The water-carbon interactions were calculated from the oxygen-carbon L-J potentials [16], as shown in Eq. (2.1). In Eq. (2.1), r is the distance between any two atoms, and σ and ε represent the zero energy separation distance and the minimum energy, respectively. The subscripts i and j are the atom indexes. By varying the coefficients, σ and ε of Lennard-Jones (L-J) potentials (Eq. (2.1)), different contact angles between droplets and the graphite substrate were mimicked. Detailed L-J coefficients under different contact angles are listed in Table 1.

$$U_{ij} = 4\varepsilon_{ij}\left[\left(\frac{\sigma_{ij}}{r_{ij}}\right)^{12} - \left(\frac{\sigma_{ij}}{r_{ij}}\right)^{6}\right]. \tag{2.1}$$

Periodic boundary conditions were applied to all three directions and a cut-off distance of 16Å was adopted. Trial simulations have been conducted to make sure that the cutoff distance in the presented simulations has no effect on the simulation results. A time step of 1fs was deemed suitable [17] and kept constant for all simulations in the present study.

Parallel equilibrium simulations of droplets and graphite substrate with different coefficients as listed in Table 1 were conducted before the collision simulations. In the equilibrium simulations, the two droplets were initially placed above the substrate with their COMs 6Å higher than the graphite surfaces (as shown in Fig. 1(a)). All equilibrium simulations were undertaken at the temperature of 300K, and the canonical ensembles (NVT) were employed. Each equilibrium simulation lasted for 2ns to ensure the equilibrium of

Table 1: Values of potential parameters [18].

atom	σ/Å	εkcal·mol^{-1}	$\theta/^\circ$
H-C	0	0	108 and 143
O-C	3.190	0.07493	108
O-C	3.190	0.04496	143

the system. Due to the different coefficients used in equilibrium simulations, the droplets and the substrate finally formed different contact angles as shown in Figs. 1(a) and (b). After equilibrium simulations, each droplet was then assigned the same impact velocity along the x direction. Meanwhile, a series of MD simulations with varying impact velocity were carried out to explore the droplet behaviours on the graphite substrate.

All the MD simulations are performed on the platform of LAMMPS [19], and carried out on ARCHER, the UK national supercomputing service. The visualisation of the molecular dynamics simulation is aided by the Visual Molecular Dynamics package [20].

3 Results and discussion

3.1 Reproduction of self-propelled jump behaviours by MD simulations

Droplet collisions on a hydrophobic substrate with a droplet-substrate contact angle of 108° were first simulated. Impact Reynolds number (Re), as defined in Eq. (3.1), was used to describe the droplet velocities and the interactions between droplets and substrate. In Eq. (3.1), ρ is the density of the droplet, namely 0.996×10^3kg/m^3. Macroscopic properties of water were selected to calculate Re numbers in Eq. (3.1). μ is the droplet dynamic viscosity, and we adopted the value of 851μpa·s [21, 22]. v and d represent the droplet impact velocity and diameter, respectively. For simplification, droplets are treated as spheres despite deformations by the substrate

$$Re=\frac{\rho v d}{\mu}. \tag{3.1}$$

In the case of $\theta=108^\circ$, we simulated droplet collisions on the graphite substrate with impact Reynolds numbers varying from 10 to 21. Results have shown that only coalescence, rather than jump of droplets, is observed after the binary droplets collide within the given Re range. The failure to reproduce the jump of droplets may be due to the weak hydrophobicity of the substrate. Thus, cases with larger contact angles, in which the substrate possesses super-hydrophobicity, was conducted.

Binary collisions were then simulated on a hydrophobic substrate with a droplet-substrate contact angle of 143° at different Reynolds numbers. When Re equals 11.7, the droplets coalesce (Fig. 3(a)) as happened in the case with the contact angle of 108°.

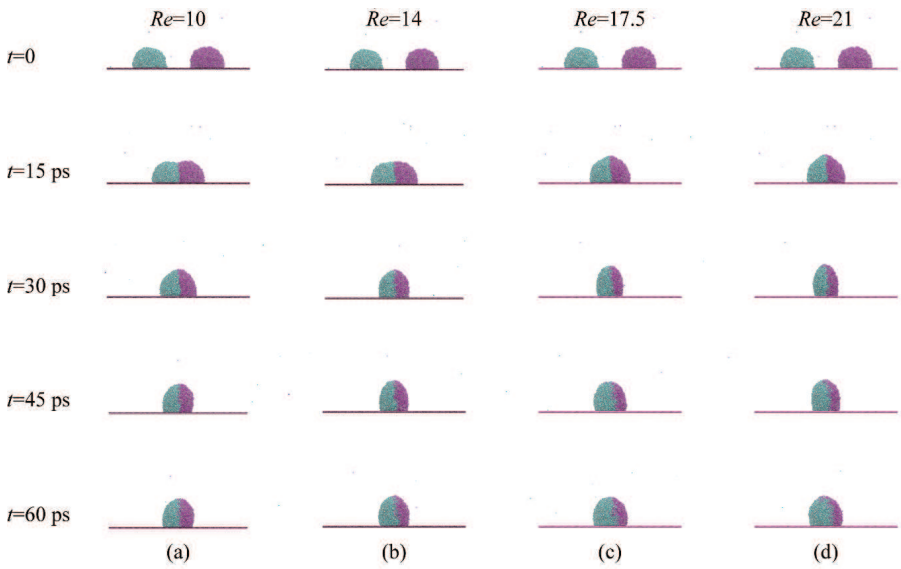

Figure 2: Droplet collisions on the substrate with contact angle of 108 degrees. Impact Reynolds number is (a) 10; (b) 14; (c) 17.5; (d) 21.

However, when Re increases to 17.5, an interesting phenomenon of the coalesced droplets jumping above the substrate was observed (Fig. 3(b)).

Three key stages can be identified in the jump process. The position of centre of mass (COM) of either separate droplet or merged droplet along the z-direction (Z_{COM}) is adopted to help understand the droplet behaviours. At the very beginning $(t=0\sim15ps)$, the two droplets approach, contact and fuse into each other. During this process, the average Z_{COM} of both droplets remains unchanged. The second stage $(t=15\sim45ps)$ is the union of the droplets and the preparation for the jump of the united droplets. As the two droplets permeate into each other, a large droplet with a peach shape is formed at $t=30ps$. Thereafter, the large repelling force from the impermeable substrate drives the basal water molecules to move upwards, thereby lifting the COM of the merged droplet and resulting in the increase of Z_{COM}. Meanwhile, the outline of the large droplet gradually changes from peach-like to rugby-like. In the last stage $(t=45\sim60ps)$, the rugby-like droplet detaches from the substrate as the COM moves upwards. Thus, this stage is also named the jump stage of the merged droplet. Since the simulations were conducted in vacuum, neither drag forces from ambient gases nor gravity of the droplet were considered. The droplet will finally move upwards at a constant velocity smaller than the impact velocity in the direction perpendicular to the substrate. Consequently, an increase in distance between the droplet and the substrate, namely Z_{COM}, can be obviously observed in the jump stage. The whole process including three aforementioned stages can spontaneously occur, so we name this process "self-propelled jump regime", which is also consistent with previous naming conventions [23].

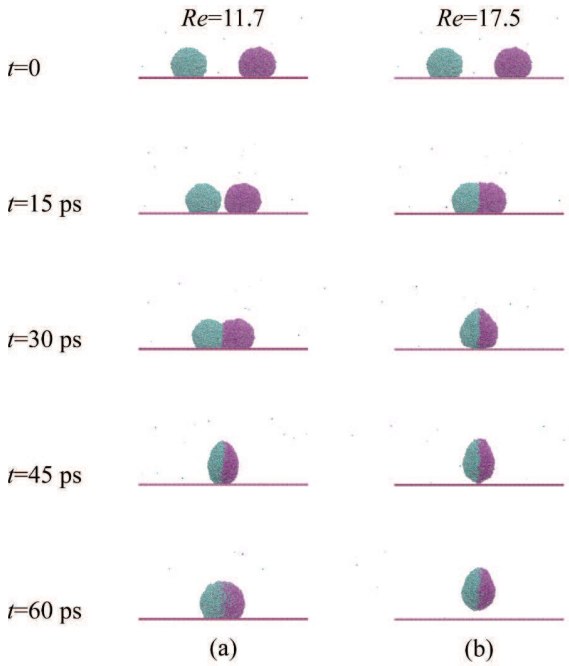

Figure 3: Droplet collisions on the substrate with contact angle of 143 degree. The impact Reynolds number is (a) 11.7; (b) 17.5.

3.2 Explanation for self-propelled jump regime

Self-propelled jump phenomena of droplets have been reported in experimental and mesoscopic studies. In these studies, Ohnesorge number (Oh) was adopted to depict the movement features, especially as a criterion to judge the occurrence of the self-propelled jump regime [24]. Oh is defined to relate the dynamic behaviours with forces and material properties, and can be calculated by Eq. (3.2), where σ represents the droplet surface tension with a value of 71.7mN/m [25]

$$Oh = \frac{\mu}{\sqrt{\rho\sigma d}}. \tag{3.2}$$

In [26], experimental and LBM studies found that self-propelled jump only occurs when Oh is smaller than 0.217 [26]. However, in the present simulation where the water droplets have diameters of 10nm and Re is 17.5, the corresponding Oh is already 1.418 while the self-propelled jump behaviours can still be observed. The discrepancy indicates that the criteria to judge the occurrence of the self-propelled jump regime from experimental and mesoscopic may not be applicable to microscopic binary collisions.

To understand the jump process in depth, we scrutinize the droplet velocity fields at key instants. To calculate the velocity distribution of droplets, we map the molecules from the Lagrangian system into the Eulerian system, which can be divided into the following steps:

a. Drawing a box that contains the calculation zoom, and cutting the box into $N_x \times N_y \times N_z$ mesh.

b. Counting number of molecules and total velocity in each cell as the number density.

c. Calculating the average velocity in each cell (total velocity divided by number of molecular).

d. Normalizing density.

When setting cell numbers, it is worth noting that the cell size should be large enough to contain at least 5 molecules for the droplet region. By using this method, instantaneous droplet velocity fields at key instants are shown in Fig. 4. In the first stage, when the two droplets are approaching each other $(t = 0 \sim 15ps)$, the orientations of droplet velocities are horizontal as expected. In the second stage $(t = 15 \sim 45ps)$ when the two droplets collided, and the kinetic energy of droplets dissipates during collision and the horizontal velocities of both droplets decrease significantly. The presence of the substrate sterically

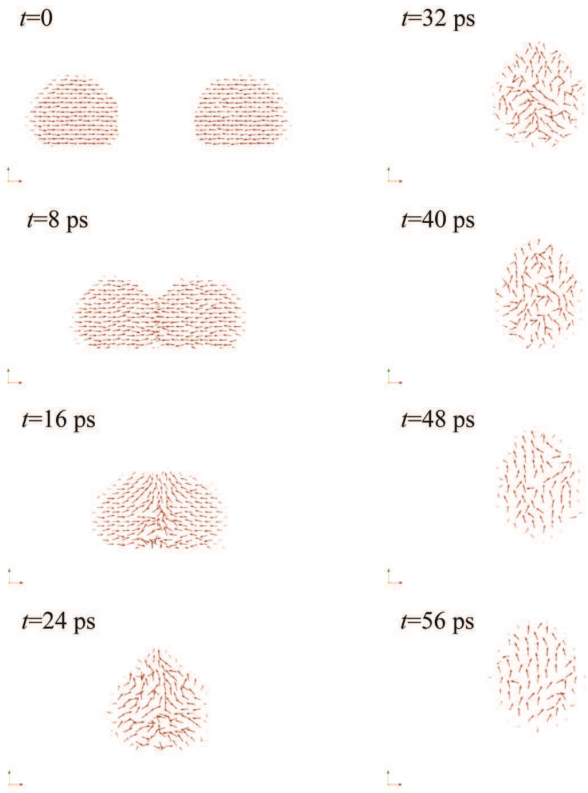

Figure 4: Droplet velocity fields during the whole jump regime process.

hinders the water molecules in the merged region to move downwards, resulting in water being stacked on the substrate surface as well as the peach-like shape of the droplet. Meanwhile, vertical velocities are generated due to the steric hindrance of substrate as well as the repelling force from substrate. In the third stage $(t = 45 \sim 60ps)$, when the rugby-like droplet detaches from the substrate, the velocity fields mostly become vertically orientated.

3.3 Influencing parameters of self-propelled jump regime

As shown previously (see Fig. 2 and Fig. 3), the contact angle and impact Reynolds number of droplets are both key parameters which may influence the droplet behaviours. Thus, parallel simulations with varying contact angles and impact Reynolds numbers have been conducted, and preliminary discussions are presented in the following section.

The values of Z_{COM} of droplets with contact angles of 143, 108 and 83 degrees and varying impact Reynolds numbers are investigated, as shown in Fig. 5.

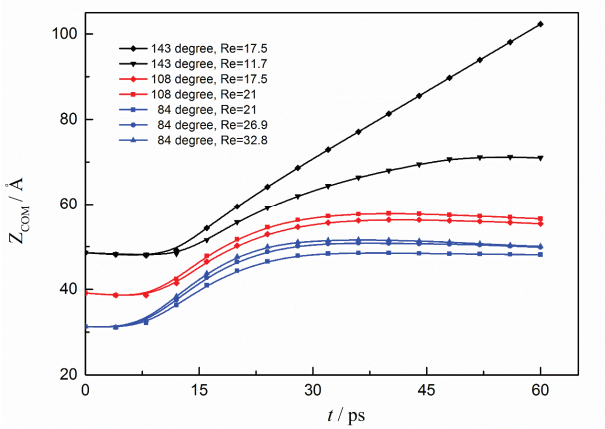

Figure 5: Z_{COM} evolution with varying contact angles and Reynolds numbers.

3.3.1 Impact Reynolds number

The two curves with contact angle of 143° in Fig. 5, together with the aforementioned in silica experimental results shown in Fig. 3, indicate that in our studies the self-propelled jump phenomenon is observed (Fig. 3(b)) only when two droplets collide on superhydrophobic substrate with a contact angle of 143° and Re of 17.5.

In the low Re case $(Re = 11.7)$, the moderate collision between two droplets results in relatively smaller deformation and correspondingly a slighter lifting of droplet COM, compared with the high Reynolds number case $(Re = 17.5)$. So in Fig. 5, the Z_{COM} curve in the case of Re being 11.7 is mostly beneath that of Re being 17.5. Meanwhile, when Re is small, the mild kinetic energy and the insufficient hindrance on droplet deformation

by the substrate fail to drive the merged droplet bounce off the substrate, so Z_{COM} curve in the case of Re being 11.7 gradually flattens as the simulation goes. Therefore, collision with high impact Reynolds numbers is a premise for the self-propelled jump of droplet.

3.3.2 Contact angle

We decrease the contact angle from 143° to 108° with the unchanged Re of 17.5. Unfortunately, no self-propelled jump phenomenon is detected with contact angle of 108°. Even though we then increase the Reynolds number to 21, self-propelled jump phenomenon does not appear either, as the red curves show in Fig. 5. However, we can still find that the increase in Reynolds number trends to lift the droplet COM higher due to the larger deformation potential after collision. For example, when $\theta = 108°$ and $Re = 21$, the Z_{COM} change between the final and the initial states is 19Å, while its $Re = 17.5$ counterpart only has a Z_{COM} increase of 17Å.

We finally conducted simulations with contact angle $\theta = 84°$ under which the graphite substrate performs hydrophilic properties with droplets. As the blue lines shows in Fig. 5, the binary collisions on the substrate only follow the coalescence rather than the self-propelled jump regime regardless of how large the Reynolds numbers are. Moreover, as expected, the Z_{COM} changes between the final and the initial states increase with Re.

Moreover, when the Reynolds number equals 21, the Z_{COM} change in the $\theta = 84°$ case is 17Å while its $\theta = 108°$ counterpart is 19Å. The smaller Z_{COM} change of $\theta = 84°$ case can be attributed to the hydrophilic properties of the substrate. The attractive interplay between the hydrophilic substrate and the droplets pulls the droplet COM towards the surface, leading to a smaller Z_{COM} increase. For this reason, it can be deduced that the self-propelled jump regime may never occur on hydrophilic surfaces.

In summary, the self-propelled jump regime only happens when binary droplet collisions take place on a super-hydrophobic surface and with high impact Reynolds numbers. Droplets moving under high impact Reynolds numbers carry large kinetic energy which can be converted into large deformation potential. Meanwhile, the super-hydrophobic substrate surface sterically hinders the deformation of droplet from permeating through the substrate; on the other hand, the repelling interactions between the super-hydrophobic substrate and the liquid molecules drive the droplet COM away from the substrate surface.

4 Conclusions

Molecular dynamics simulations of droplet collisions on graphite substrates with different contact angles and Reynolds numbers have been conducted. The self-propelled jump phenomenon of nanoscale droplets has been reproduced for the first time by MD. Results show that binary droplet collisions with high impact Reynolds numbers on super-hydrophobic substrates are most likely to lead to the self-propelled jump phenomenon. Furthermore, parametric studies indicate that the criterion based on the Oh number de-

rived from the mesoscopic self-propelled jump regime is insufficient to precisely predict a nanoscale self-propelled jump phenomenon. The present study shows that the impact Reynolds number and the substrate properties like contact angle should serve as additional criteria for the occurrence of the self-propelled jump behaviours. In further investigations, a complete regime map and criteria for predicting nano-scale droplet collision and jump behaviours on substrates will be developed. Finally, it is worth pointing out that MD can only be used to investigate a system with nano-droplets due to the limitation imposed by computational cost considerations. On the other hand, experimental results on self-propelled droplet jump have employed micro-droplets. There is therefore no direct comparison between our MD results and experimental observations. Nevertheless, it is quite reassuring that MD has shown the existence of self-propelled jump of nano-droplets, which should be due to the same mechanism as that behind the self-propelled jump of micro-droplets. It is hoped that future experimental work will confirm our findings.

Acknowledgments

The authors gratefully acknowledge the support from the Major Project of the National Science Foundation of China (Grant No. 91441120) and the Center for Combustion Energy at Tsinghua University. The simulations were performed on the UK National Supercomputing Service ARCHER funded under the EPSRC Grant No. EP/J016381/1 and No. EP/L00030X/1.

References

[1] J. B. Boreyko and C. H. Chen, Self-propelled dropwise condensate on superhydrophobic surfaces, Phys. Rev. Lett., 103(18) (2009), 4501–4501.
[2] R. Helbig, J. Nickerl, C. Neinhuis and C. Werner, Smart skin patterns protect springtails, Plos One, 6(9) (2011), 120–120.
[3] J. A. Watson, B. W. Cribb, H. M. Hu, and G. S. Watson, A dual layer hair array of the brown lacewing: repelling water at different length scales, Biophys. J., 100(4) (2011), 1149–55.
[4] R. Enright, N. Miljkovic, A. Alobeidi, C. V. Thompson, and E. N. Wang, Condensation on superhydrophobic surfaces: the role of local energy barriers and structure length scale, Langmuir the Acs Journal of Surfaces & Colloids, 28(40) (2012), 14424–32.
[5] J. B. Boreyko, and C. P. Collier, Delayed frost growth on jumping-drop superhydrophobic surfaces, Acs Nano, 7(2) (2013), 1618–1627.
[6] K. M. Wisdom, J. A. Watson, X. Qu, F. Liu, G. S. Watson and C. H. Chen, Self-cleaning of superhydrophobic surfaces by self-propelled jumping condensate, Proceedings of the National Academy of Sciences of the United States of America, 110(20) (2013), 7992–7.
[7] F. C. Wang, F. Yang and Y. P. Zhao, Size effect on the coalescence-induced self-propelled droplet, Appl. Phys. Lett., 98(5) (2013), 053112–053112–3.
[8] J. B. Boreyko and C. H. Chen, Vapor chambers with jumping-drop liquid return from superhydrophobic condensers, Int. J. Heat Mass Transfer, 61(1) (2013), 409–418.

[9] T. Q. Liu, W. Sun, X. Y. Sun and H. R. Ai, Mechanism study of condensed drops jumping on super-hydrophobic surfaces, Colloids Surfaces A Physicochem. Eng. Aspects, 414(46) (2012), 366–374.
[10] B. Peng, S. Wang, Z. Lan, W. Xu, R. Wen and X. Ma, Analysis of droplet jumping phenomenon with lattice boltzmann simulation of droplet coalescence, Appl. Phys. Lett., 102(15) (2013), 151601–151601–4.
[11] J. C. Pothier and L. J. Lewis, Molecular-dynamics study of the viscous to inertial crossover in nanodroplet coalescence, Phys. Rev. B, 85(11) (2012), 117–122.
[12] W. L. Jorgensen, J. Chandrasekhar, J. D. Madura, R. W. Impey and M. L. Klein, Comparison of simple potential functions for simulating liquid water, J. Chem. Phys., 79(2) (1983), 926–935.
[13] A. D. MacKerell, D. Bashford, M. Bellott, R. L. Dunbrack, J. D. Evanseck, M. J. Field, S. Fischer, J. Gao, H. Guo, S. Ha, D. Joseph-McCarthy, L. Kuchnir, K. Kuczera, F. T. K. Lau, C. Mattos, S. Michnick, T. Ngo, D. T. Nguyen, B. Prodhom, W. E. Reiher, B. Roux, M. Schlenkrich, J. C. Smith, R. Stote, J. Straub, M. Watanabe, J. Wiorkiewicz-Kuczera, D. Yin and M. Karplus, All-atom empirical potential for molecular modeling and dynamics studies of proteins, J. Phys. Chem. B, 102(18) (1998), 3586–3616.
[14] J. V. L. Beckers, C. P. Lowe and S. W. De Leeuw, An iterative PPPM method for simulating Coulombic systems on distributed memory parallel computers, Mol. Simul., 20(6) (1998), 369–383.
[15] S. L. Price, A. J. Stone and M. Alderton, Explicit formulas for the electrostatic energy, forces and torques between a pair of molecules of arbitrary symmetry, Mol. Phys., 52(4) (1984), 987–1001.
[16] L. Verlet, Computer experiments on classical fluids I. Thermodynamical properties of Lennard-Jones molecules, Health Phys., 22(1) (1967), 79–85.
[17] X. Z. Jiang, Y. R. Zhang and K. H. Luo, Dynamics of nano-cluster collisions in carbon nanotubes, J. Nanosci. Nanotech., 16(8) (2016), 8380–8386.
[18] T. Werder, J. H. Walther, R. L. Jaffe, T. Halicioglu and P. Koumoutsakos. On the watercarbon interaction for use in molecular dynamics simulations of graphite and carbon nanotubes, J. Phys. Chem. B, 107(6) (2003), 13345–1352.
[19] S. J. Plimpton, Fast parallel algorithms for short-range molecular dynamics, J. Comput. Phys., 117 (1995), 1–19.
[20] W. Humphrey, A. Dalke and K. Schulten. VMD: visual molecular dynamics. J. Mol. Graph., 14 (1996), 33–38.
[21] L. Haar, NBS/NRC Steam Tables, (CRC Press, 1984).
[22] J. Sengers and J. T. R. Watson, Improved international formulations for the viscosity and thermal conductivity of water substance, J. Phys. Chem. Ref. Data, 15(4) (1986), 1291–1314.
[23] Y. R. Zhang, X. Z. Jiang and K. H. Luo. Bounce regime of droplet collisions: a molecular dynamics study, J. Comput. Sci., 2016.
[24] L. Fangjie, G. Ghigliotti, Giovanni, J. J. Feng and James, Self-propelled jumping upon drop coalescence on leidenfrost surfaces, J. Fluid Mech., 752 (2013), 22–38.
[25] N. Vargaftik, B. Volkov and L. Voljak, International tables of the surface tension of water, J. Phys. Chem. Ref. Data, 12(3) (1983), 817–820.
[26] F. Liu, G, Ghigliotti, J. J. Feng and C. H. Chen. Numerical simulations of self-propelled jumping upon drop coalescence on non-wetting surfaces, J. Fluid Mech., 752 (2014), 39–65.